New LOFAR discovery of a hybrid radio halo in the galaxy cluster Abell 1413

Giulia Lusetti, *A. Bonafede, L. Lovisari, M. Gitti, R. Cassano, S. Ettori, F. de Gasperin*

ABSTRACT

Abell 1413 is a massive ($M_{500} = 5.99^{+0.46}_{-0.45}\, 10^{14}\, M_\odot$), nearby ($z = 0.1427$), hot ($kT = 6.98^{+0.07}_{-0.06}$ keV) galaxy cluster. In this work, XMM-Newton data were used to investigated the dynamical status of Abell 1413. X-ray observations show that the system is not undergoing mergers and does not have a disturbed morphology. X-ray analysis suggests instead that this Abell 1413 is a weak-cool-core cluster, i.e., not a completely relaxed system, that could have experienced a past of minor mergers.

LOFAR observation at 144 MHz has revealed a large-scale radio source never detected before in the galaxy cluster Abell 1413. In contrast to what has been generally believed, cluster-scale radio emission has also been observed in clusters with no sign of major mergers, indicating that minor mergers and/or sloshing of a dense cool core could trigger particle acceleration on larger scales and generate steep-spectrum radio emission. In fact, respect to what previously found, Abell 1413 not only hosts a mini-halo centred source, but also a low surface brightness more extended radio source on scale of ~800 kpc (N-S direction). We classify the extended radio emission as a superposition of two different sources: the more compact mini-halo emission, at the cluster centre; surrounded by a low-brightness giant-halo on larger scales. To validate this hypothesis, we performed an integrated spectral analysis and point-to-point correlation between the X-ray and radio surface brightness.

Conclusion. We argue that the presence of diffuse radio emission on the cluster scale is consistent with the scenario of a minor merger event, not powerful enough to significantly perturb the core. This turbulent event has created the extended radio halo emission without destroying the cool core: cooling region $r_{cool} <$ 90 kpc with $t_{central,cool} \sim$ 6 Gyr (week-cool-core system). The coexistence of two different kinds of radio emission is suggested by different spectral index: $\boldsymbol{\alpha_{mini\text{-}halo} = 1.1 \pm 0.2}$ vs $\boldsymbol{\alpha_{halo} > 1.6}$ ($S_\nu \propto \nu^{-\alpha}$) and different X-ray and radio surface brightness correlations (**sub-linear** and **super-linear** for the mini-halo and giant-halo, respectively), indicating distinct mechanisms of particles acceleration.

1) X-ray analysis: dynamical status

Surface brightness profile

$$S(r) = S_{0,1}\left[1+\left(\frac{r}{r_{c,1}}\right)\right]^{-3\beta_1+0.5} + S_{0,2}\left[1+\left(\frac{r}{r_{c,2}}\right)\right]^{-3\beta_2+0.5}$$

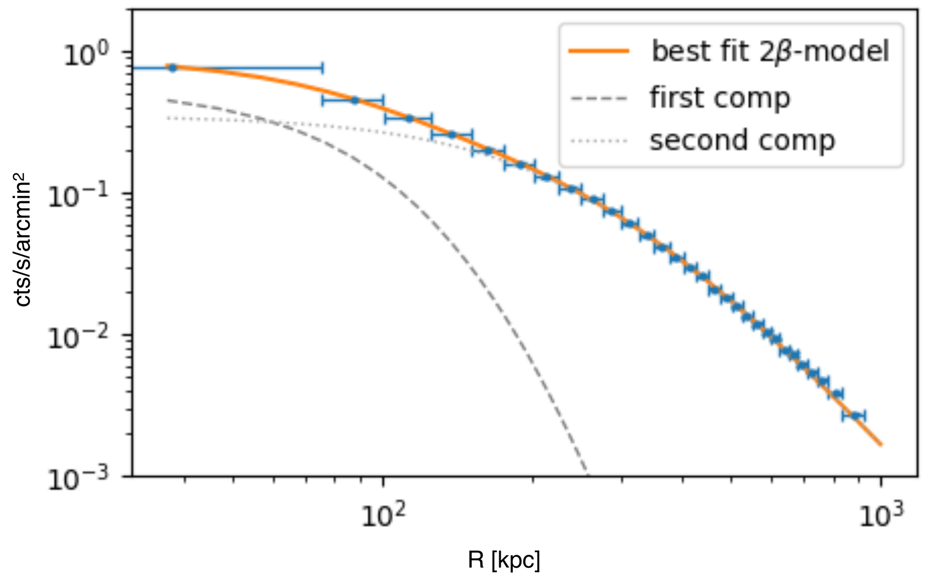

Surface brightness profile fitted with the best fit double β model: the two components are visible as dotted and dashed grey line. Best fit parameters: $\Sigma_{01} = 0.56 \pm 0.05, r_{c1} = 189.62 \pm 0.41, \beta_1 = 2.17 \pm 0.91$ and $\Sigma_{02} = 0.35 \pm 0.04, r_{c2} = 257.04 \pm 0.25, \beta_2 = 0.80 \pm 0.04$.

Surface brightness profile is well fitted with a double β-model, which typically accounts for brightness excess in the central core of cool- core relaxed systems.

Cooling time profile

$$t_{cool} = \frac{H}{\Lambda(T) n_e n_p}$$

$$1\, Gyr < \mathbf{t_{cool,central}} \sim \mathbf{6\, Gyr} < 7.7\, Gyr \sim t_{age}$$

with t_{age} look-back time at z=1, because at this time many clusters appear to be relaxed

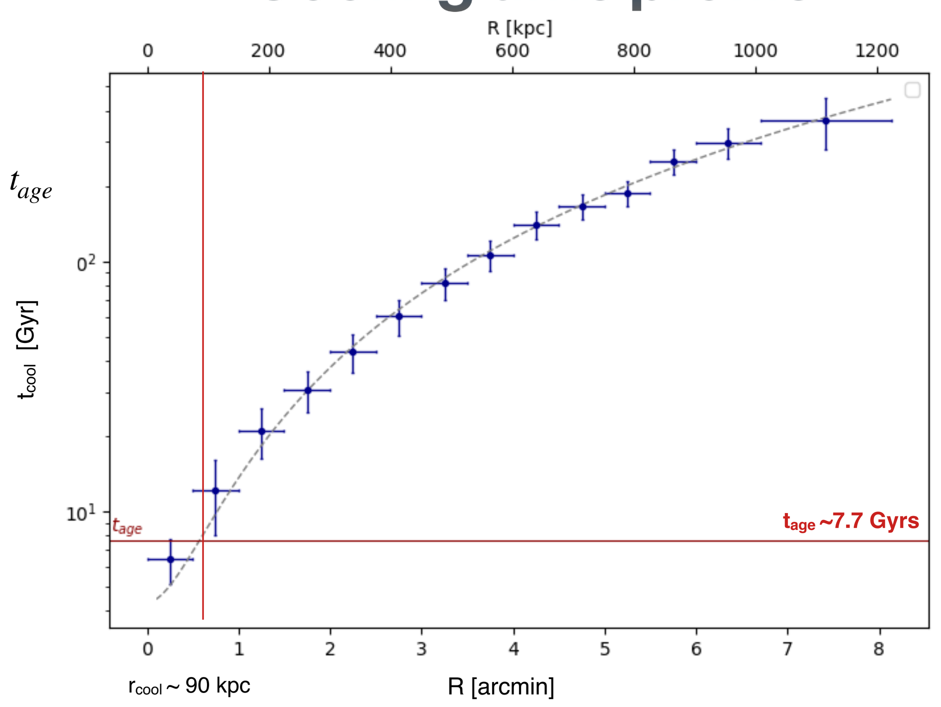

Cooling time profile for A1413. Each point represents the cooling time for a given annular region used for the spectral extraction. The red line represents t_{age} = 7.7 Gyr while the grey line is the best fit $t_{cool} = 9.26 r^{1.84}$.

Weak cool-core clusters are characterized by moderate cooling time, elevated central entropy, and slightly decreasing central temperature profiles (Hudson et al. 2010).

2D temperature map

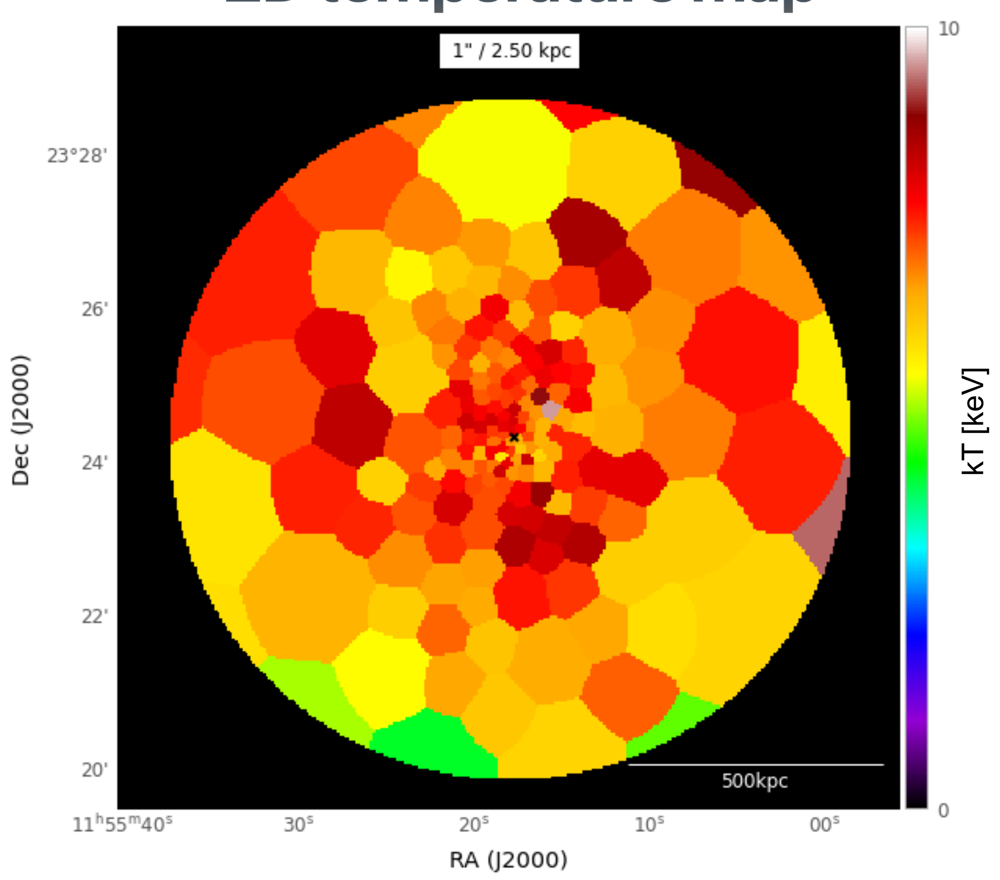

2D temperature map centered in Xray peak, obtained with S/N=50 and within $0.5\, R_{500}$.

Local variations of the temperature are found, that could be due to past minor or major merger events. The presence of diffuse radio emission on the cluster scale is consistent with the scenario of a minor merger event, *not* powerful enough to significantly perturb the core.

2) Radio images at 144MHz (LOFAR HBA)

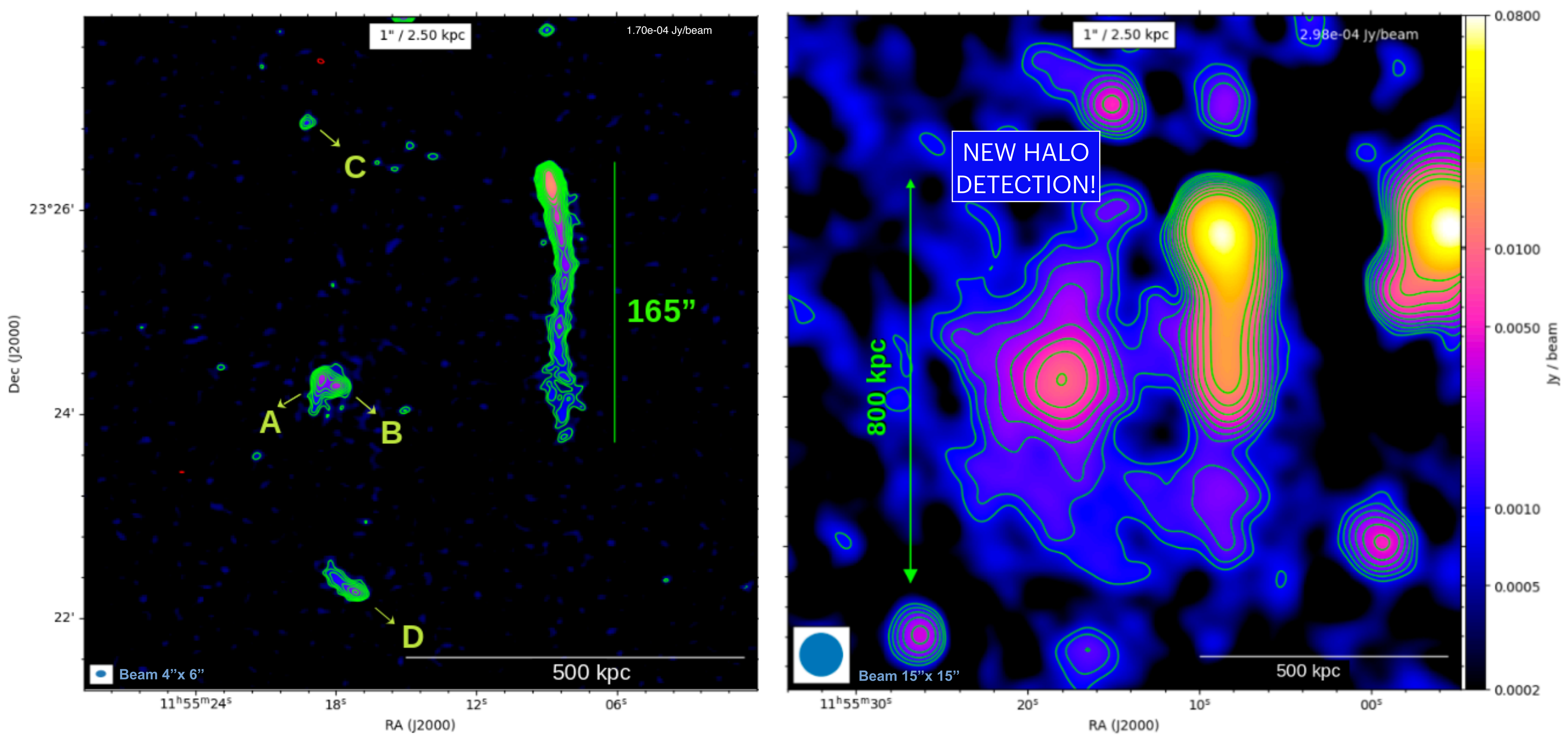

Left: High resolution 144 MHz image with beam 4″ × 6″. The contour levels start at 3σ, where σ = 170 µJy/beam, and are spaced with a factor of √2. Point sources labeled with letters have been subtracted subtracted. **Right:** Low resolution 144 MHz image with beam 35″ × 35″. The contour levels start at 3σ, where σ = 298 µJy/beam, and are spaced with a factor of √2.

References:

Govoni, F. et al. (2001), "A comparison of radio and X-ray morphologies of four clusters of galaxies containing radio halos", A&A

Govoni, F. et al. (2009), "A search for diffuse radio emission in the relaxed, cool-core galaxy clusters A1068, A1413, A1650, A1835, A2029, and Ophiuchus", A&A

Savini F. et al. (2018), "A LOFAR study of non-merging massive galaxy clusters", A&A

Ignesti A. et al. (2020), "Radio and X-ray connection in radio mini-halos:implications for hadronic models", A&A

Botteon, A. et al. (2020), "The beautiful mess in Abell 2255", A&A

3) Higher frequency VLA data at 1.4 GHz

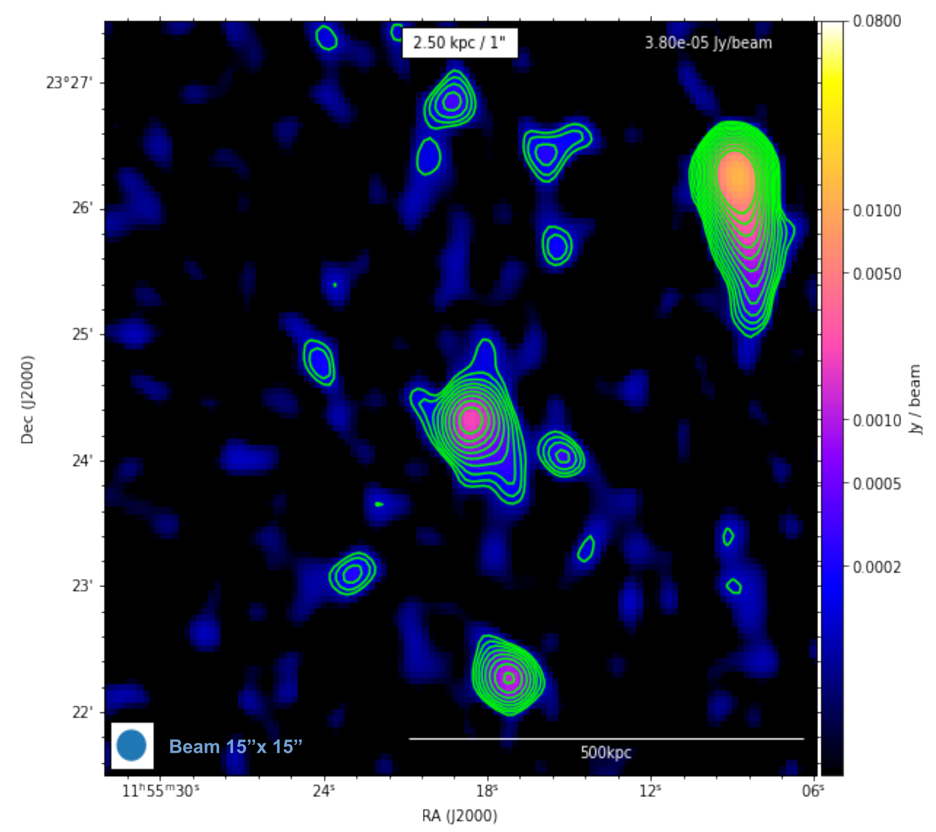

Image of A1413 from Govoni et al. (2009) at 1.4 GHz with a FWHM of 15″ × 15″. The first contour level is drawn at 0.1 mJy/beam and the rest are spaced by a factor of √2.

Integrated spectral index of **central mini-halo** region

$$\alpha_{144}^{1.4} = 1.1 \pm 0.2$$

(typical of mini-halo)

1σ limit for the **halo** emission

$$\alpha_{144}^{1.4} > 1.6$$

steep spectrum extended emission

4) Point-to-point correlation

Point-to-point comparison between radio and X-ray surface brightness. Data are then fitted with a generic power-law relation of the type

$$\log I_R = A \, \log I_X + B$$

where the slope of the scaling A determines whether the radio brightness (i.e. the mag- netic field strength and CRe density) declines faster ($A > 1$) than the X-ray brightness (i.e. the thermal gas density), or vice versa ($A < 1$).

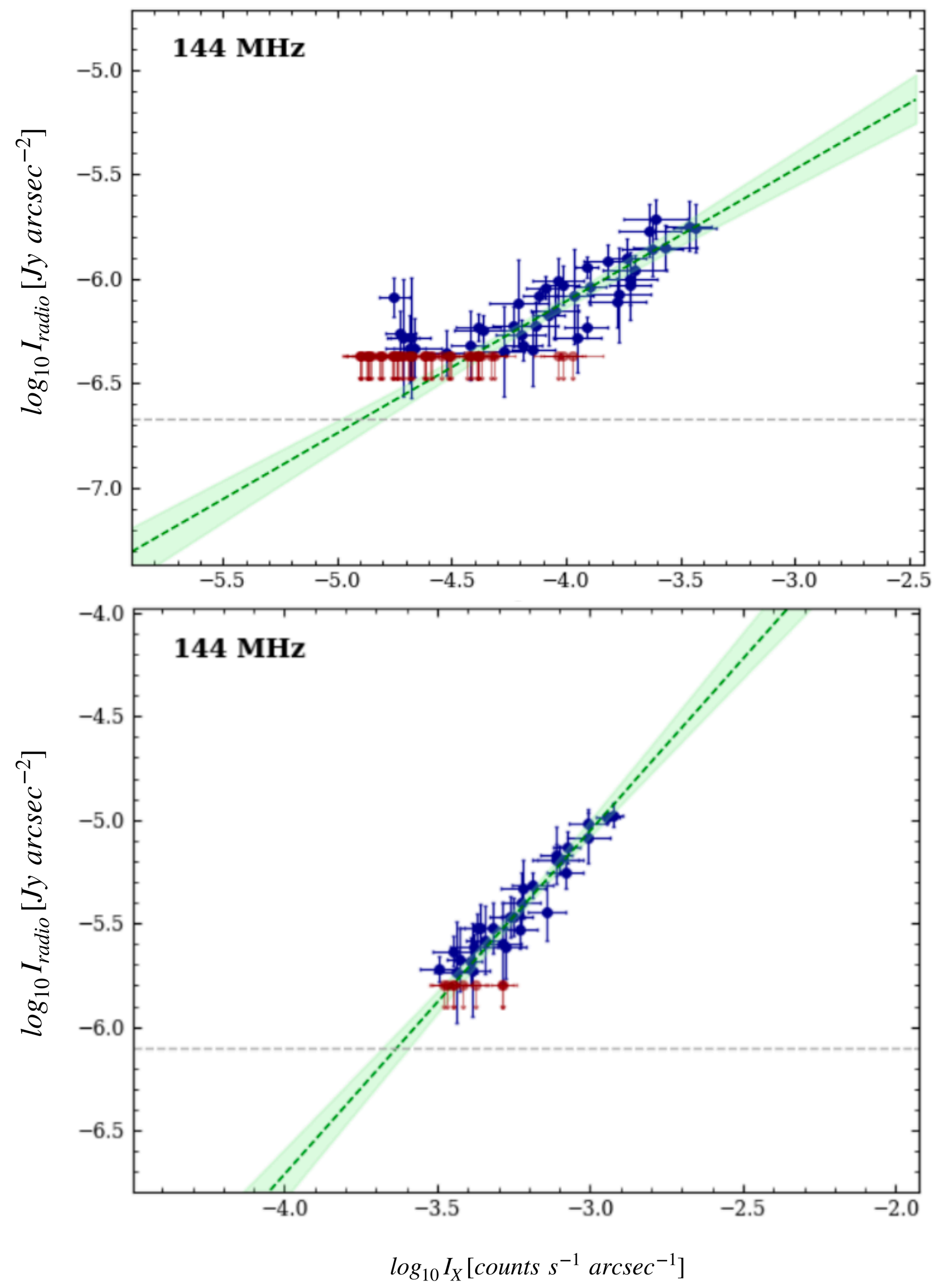

The giant-halo emission shows a **sub-linear relation**

$$I_R \propto I_X^{0.63^{+0.07}_{-0.06}}$$

The mini-halo emission shows a **super-linear relation**

$$I_R \propto I_X^{1.66^{+0.16}_{-0.13}}$$

$I_R - I_X$ relation of the giant-halo (top) and mini-halo (bottom) in A1413, extracted in square boxes with width of 35″ and 15″ respectively. The radio brightness strongly correlates with the X-ray. In both plots, upper limits (dark-red points with arrow) refer to cells where the radio surface brightness is below the 2σ level. Shaded green area show samples from the posterior distribution. The best-fit (green dashed line) is reported with the corresponding 1σ confidence interval.